Research Article

Handan Aydın, Ecem Özen Öner and Cihat Aydın*

Role of tungsten oxide (WO_3) on thermal and optical properties of smart polymer composites

https://doi.org/10.1515/phys-2025-0253
Received July 7, 2025; accepted October 27, 2025;
published online December 23, 2025

Abstract: Tungsten oxide, a versatile transition metal with numerous polymorphs and sub-stoichiometric compositions, containing inherent tunnels and oxygen vacancies, has become a current field of study due to its rich crystal structure, high electrochemical stability, easy accessibility, and environmental friendliness. Thus, the versatile structure of WO_3-based materials makes them promising candidates for advanced applications. Our study aims to provide valuable insights into the performance of these materials used in various fields. The structural, optical, and thermal characteristics of PVC-PCL composites doped with tungsten oxide (WO_3) were examined in this work. According to DSC research, the thermal characteristics of the polymer matrix were significantly impacted by the addition of WO_3. The thermal stability was found to have increased based on the TGA measurement findings. XRD analyses revealed that as the doping rate increased, improved crystallinity was seen. According to SEM tests, the grain clusters are uniformly mixed and the tungsten oxide is evenly spread across the surface. The dopant reacted either chemically or physically with the polymer matrix, according to the ATR-FTIR spectra of PVC-PCL matrix nanocomposite films. An improvement in conductivity with an increase in dopant concentration was noted in the optical experiments. Thus, it can be stated that PVC-PCL composites doped with WO_3 can be used in optoelectronic, various industrial, and biomedical application areas due to their structural, optical, and thermal properties.

Keywords: tungsten oxide (WO_3); polyvinyl chloride (PVC); polycaprolactone; composite; optical property

1 Introduction

Polymeric composites, which are seen as a versatile and innovative research topic, have provided advantages compared to other materials with many features such as tunability of physical and chemical properties, flexibility, biocompatibility and eco-friendliness. Due to these properties of polymeric composites, they have been preferred in many fields such as microwave absorption layers [1], electrochromic devices [2], proton exchange membranes [3], chromatic sensors [4], capacitors [5] and Metal/Insulator/Semiconductor (MIS) photodetectors [6, 7]. Additionally, because of their low cost, good flexibility, lightweight, quick industrial processing, feasibility, ease of production, and high durability, they have recently been the subject of much research, generating a great deal of curiosity among scientists [7–9]. Polymers with important physicochemical properties are active or passive components for optical-electronic devices [10]. For their optical properties, they can be used as optical waveguide components, photochromic materials, field effect transistors, photovoltaic cells, light-generating diodes and high refractive index films. The main advantage of choosing mostly polymers is that the addition of additives significantly extends the range of physical parameters compared to pure polymer. The material's qualities may become more favorable for certain uses. Many scientific studies have shown that doped polymer materials have improved processability [11]. Many polymer types such as polymethyl methacrylate (PMMA), polyvinyl alcohol (PVA), polyvinyl chloride (PVC), polyvinyl pyrrolidone (PVP), polyaniline (PANI) and poly(3,4-ethylene dioxythiophene) polystyrene sulfonate (PEDOT:PSS), poly(lactic acid) (PLA) are used for

***Corresponding author: Cihat Aydın**, Department of Airframe and Powerplant Maintenance, School of Civil Aviation, Firat University, Elazığ, Türkiye, E-mail: caydin@firat.edu.tr.
https://orcid.org/0000-0001-9997-6326
Handan Aydın, Department of Medical Services and Techniques Optician Program, Munzur University, Tunceli, Türkiye.
https://orcid.org/0000-0002-0141-9773
Ecem Özen Öner, Department of Physics, Faculty of Science, Firat University, Elazığ, Türkiye

these purposes [7]. Among these various polymer types, Poly(vinyl chloride) (PVC) is one of the most widely used thermoplastic polymers due to its multipurpose properties and low cost [12]. PVC, the third most widely known polymer worldwide, is closely related to human life as it is used in many fields such as clothing, construction materials, medicine, automobiles and many more. It is highly preferred for its excellent properties such as high transparency, easy maintenance and non-flammability [13]. PVC, which contains a very low percentage of additives, exhibits inherent flame resistance through the release of hydrogen chloride gas, which is non-flammable at high temperatures [14, 15]. Used in the medical industries, PVC is even used in sterilizable blood storage bags, a testament to its good mechanical properties and excellent transparency [13]. WO_3 nanoparticles contribute unique optical and photocatalytic properties, along with thermal stability and high electron mobility. unique optical and PCL ($C_6H_{10}O_2$) is a semi-crystalline aliphatic polymer with excellent compatibility with PVC. Synthesized in the early 1930s, PCL has become a source of intense interest day by day. PCL, which is biocompatible and biodegradable, is a hydrophobic, semi-crystalline compound with monomer unit ε-caprolactone, melting point between 59–64 °C and glass transition temperature – 60 °C. These characteristics make processing it simple. PCL readily dissolves in organic solvents like tetrahydrofuran (THF) and chloroform, and as its molecular weight rises, its crystallinity tends to diminish [16].

One efficient way to alter a material's morphological characteristics, physical attributes, and chemical behavior is to include mineral trioxide into a polymeric composition [17]. Tungsten oxide (WO_3), an n-type semiconductor metal oxide, has long diffusion length, high electron affinity, high work function ($\Phi > 6$ eV). WO_3 contributes to a wide range of applications in optical modulation devices, electrochromic devices, photochromic materials, photocatalysts, smart windows, gas sensing applications, detection of malaria biomarkers and many more [7, 18]. By adjusting to the dielectric constant differential between the formed functional component and the polymeric chain, WO_3 minimizes the interfacial contact linked to Maxwell–Wagner–Sillars polarization and hence lowers leakage current. Its band gap is between 2.6 and 2.8 eV, and because of the oxygen vacancy defects in the lattice structure, the non-stoichiometric material develops a donor level, which results in intrinsic conductivity [17, 18]. The most common color of WO_3 is brown, blue and lemon yellow [18]. Substantial advantages have been realized for flexible electronic components and devices, especially within the domain of organic electronics, due to comprehensive research conducted on metal oxide semiconductors in polymer nanocomposites. The use of tungsten trioxide (WO_3) as a nanofiller, in conjunction with various polymeric matrices, is a prevalent method for the development of multifunctional polymer nanocomposites and polymer nanodielectric materials [19, 20]. In comparison to other conductive materials like Fe_2O_3, $BiVO_4$, and TiO_2, this specific material (WO_3) offers numerous benefits. To begin with, it possesses a relatively common elemental composition, rendering it more accessible and economical. Furthermore, it exhibits significant physicochemical properties, including a moderate bandgap between 2.5 and 2.8 eV, outstanding electrical characteristics, and exceptional stability in acidic solutions [21]. The incorporation of mineral trioxide into the co-polymeric mixture represents an effective strategy for altering the morphological characteristics, physical attributes, and chemical properties, thereby facilitating industrial applications [22]. Examples of such industrial applications include the production of sensors, lubricants, and catalysts. Given the optical characteristics of tungsten trioxide (WO_3), it has the capacity to absorb approximately 12 % of the incoming sunlight [23]. There are several limitations associated with the transport and separation of tungsten trioxide. Therefore, recent research suggests that integrating it into inorganic/organic nanocomposites is an advantageous method to enhance its efficiency [19]. Consequently, our study seeks to investigate possible uses in optoelectronic devices by concentrating on their thermal, structural, and optical characteristics. The difference between this study and other research is that it aims to create an ideal polymer base and improve the optical properties and various physical properties of the resulting smart polymer-based composite material by adding WO_3 to it. This will provide a different perspective on the evaluation of smart polymer composites. Most recent studies have focused on ergonomic and economical materials to make our lives easier. Thus, producing polymers that are cost-effective and lightweight, in addition to the smart properties of the prepared samples, is considered a distinctive feature in providing multiple properties in a single material [24, 25].

In this study, we focused on the potential for employing WO_3 to improve the optical and electrical characteristics of polymer blend films. Therefore, the structural, optical and thermal properties of PVC-PCL nanocomposite samples containing WO_3 nanoparticles were investigated.

2 Experimental method

In this investigation, 75 wt% poly(ε-caprolactone) (PCL) was weighed and stirred in 10 ml Tetrahydrofuran (THF) solvent

within a beaker for approximately 2 h. Concurrently, 25 wt% poly(vinyl chloride) (PVC) was weighed and subjected to the same procedure in a separate beaker. The resulting mixtures were then combined and dispersed in an ultrasonic homogenizer for 1 h to facilitate homogenization of the chemical reactions. WO_3 additives were weighed in various ratios and mixed in a magnetic stirrer at a speed of 500–600 rpm for 1 h at room temperature. Subsequently, 5 %, 10 %, 15 % and 20 % WO_3 was incorporated into homogenously dispersed PCL-PVC polymers and further dispersed for 1 h. The mixture was then subjected to a drying process in an oven at 40 °C for 24 h. Measurements of temperature-dependent phase transformations and mass changes of the generated composites were conducted at a heating rate of 10 °C/min in a pure nitrogen gas atmosphere using Perkin Elmer Sapphire differential scanning calorimetry (DSC) and Hitachi thermogravimetric analysis (TGA) instruments. FTIR spectra were collected within the wavelength range of 4,000–500 cm^{-1} using the Nicolet IS5 FTIR instrument. X-ray measurements were performed to investigate the crystal structure of all prepared samples using an X-ray analysis system (Rigaku RadB-DMAX II), applying CuKα radiation at room temperature with a voltage of 40 kV and a current of 15 mA. The surface properties of the samples were then investigated using a ZEISS brand scanning electron microscope (SEM) operated at an accelerating voltage of 25 kV. The optical spectra of the polymer composites were recorded over a wavelength range of 200–900 nm using a Perkin Elmer ultraviolet-visible (UV/VIS) spectrometer.

3 Result and discussions

DSC (Differential Scanning Calorimetry) analysis was carried out to investigate the effect of adding WO_3 nanoparticles at different rates (5 %, 10 %, 15 % and 20 %) to PVC-PCL matrix composites on thermal transition behaviors. The obtained results are given in Figure 1. Samples were analyzed in the temperature range of 0–200 °C with a heating rate of 10 °C/min. The dips in the DSC graph signify endothermic processes, while the peaks denote exothermic processes. In the obtained DSC thermograms, it was observed that the melting temperature of the pure PVC-PCL blend was approximately in the range of 60–70 °C and the location and intensity of these peaks changed with the addition of WO_3 [24, 26–28]. As the WO_3 content increased, a decreasing trend was observed in the melting peak enthalpies, which restricted the crystallization behavior of the nanoparticles in the matrix phase and showed that the crystal structure was disrupted. These results reveal that

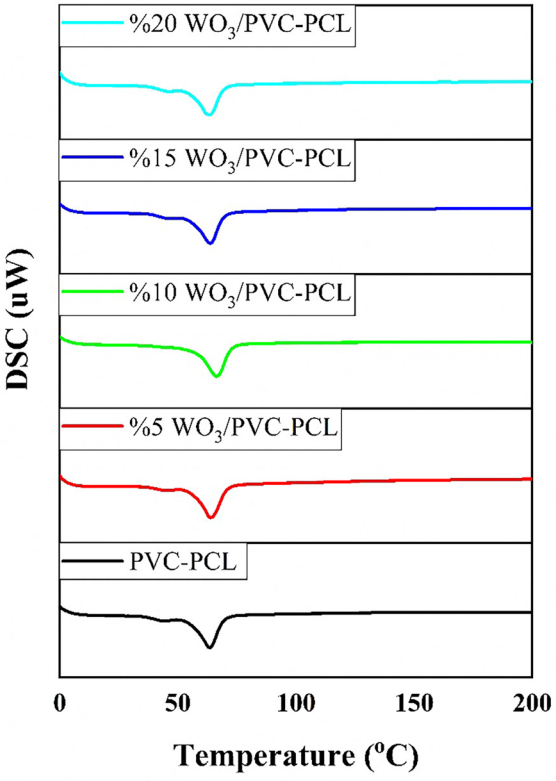

Figure 1: DSC curves of PCL-PVC composite.

WO_3 addition has a significant effect on the thermal properties of the polymer matrix. According to a recent study on WO_3/PLA, adding a specific amount of WO_3 improved crystallinity, but at higher concentrations, disorder caused the crystallinity to decline [29]. The DSC behavior of our WO_3-PVC/PCL system shows that nano-sized fillers reduce ΔH_m and raise T_g (or restrict mobility). T_g shifts and crystallinity decreases, for instance, are characteristics of filler-polymer interactions in PVC nano-additives [30]. The DSC curves shows that a decrease in the crystallinity of the PCL domains within the PVC-PCL matrix correlates with a decrease in melting enthalpy (ΔH_m) as the WO_3 content increases. The reason for this behavior is because the WO_3 nanoparticles prevent crystal formation by interfering with the usual arrangement of polymer chains [31, 32].

The TGA analysis reveals the effects of adding WO_3 nanoparticles at different rates (5 %, 10 %, 15 % and 20 %) to PVC-PCL matrix composites on thermal degradation behavior. The obtained data are given in Figure 2. In the pure PVC-PCL sample, the main degradation occurred in the range of approximately 350–480 °C and a serious mass loss was observed in this range. In the WO_3-added samples, a slight increase in the degradation temperature and a significant increase in the amount of residue occurred. In particular, the composite containing 20 % WO_3 showed the highest

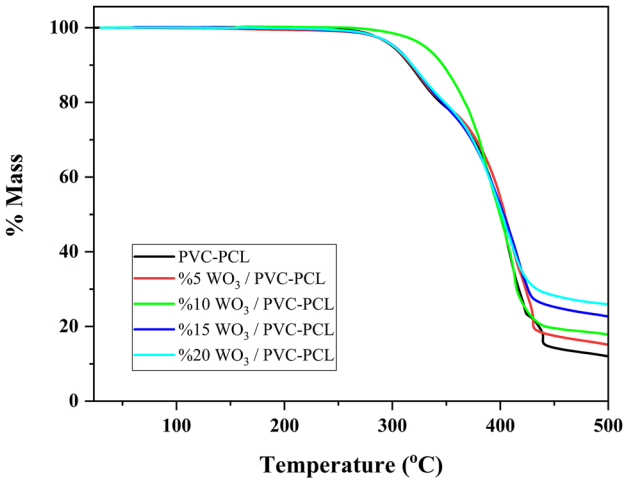

Figure 2: TGA curves of PCL-PVC composite.

degradation resistance and the highest residual mass. This shows that WO_3 nanoparticles increase thermal stability and provide resistance to thermal degradation of the polymer matrix. In addition, the later onset of thermal degradation with increasing WO_3 ratio can be associated with the effect of nanoparticles in regulating heat transfer and slowing down the degradation mechanism. The findings confirm that WO_3 addition improves the thermal resistance of the composite material and provides stability at high temperatures. It is observed that the decomposition temperatures increase as the WO_3 ratio increases. This shows that WO_3 contributes to the thermal stability of the matrix. Since WO_3 is an inorganic structure, it directly contributes to the amount of residue remaining after decomposition. The highest residual mass value (~21 %) was obtained in the sample containing 20 % WO_3. In addition, the degradation behavior of the polymer was delayed with the increase in the nanoparticle ratio, which showed that the thermal stability increased. When we examined the mass change of oxide-added polymeric composites against temperature, which we have done before, it was observed that the amount of residue increased as the oxide addition increased [33–37].

X-ray diffraction measurements were taken at room temperature to investigate the crystal structures of WO_3 doped PVC-PCL blends and are shown in Figure 3. X-ray patterns of pure PCL-PVC composite and 15 % WO_3 doped PCL-PVC composites were analyzed to better visualize the WO_3 doping. In the light of the literature data for the pure polymer blend, it is seen that two known peaks are formed. Since polyvinyl chloride shows an amorphous structure, it cannot be expected to show crystalline properties. PCL, on the other hand, is a biodegradable polyester with a semi-crystalline structure. Therefore, X-ray analysis shows diffraction peaks belonging to the (110) and (200) planes of the orthorhombic crystal phase [24, 35, 36]. It was observed that new peaks were formed with increasing doping ratio. It was observed that the number and intensity of diffraction peaks increased as the doping ratio of WO_3 doped polymer composites increased. With this result, it can be said that the crystallinity level increases for this prepared composite. Stated differently, the narrow peaks and high intensity produced show that the WO_3-doped polymer composite has good crystallinity. In other words, the high intensity and narrow peaks obtained reflect the good crystallinity of the WO_3 doped polymer composite. The crystal indices (011), (002), (020), (200), (120), (112), (022), (202), (122), (222), (004), (040), (114), (420), (340) of the monoclinic phase of WO_3 are associated with JCPDS card 83-0950. The intense diffraction peak at 22.8° corresponding to the (002) plane indicates that WO_3 crystals preferentially grow in the (200) direction [38]. KOK et al. conducted a similar study and produced La_2O_3 doped PS-PVC/PCL ternary recyclable composites and found that crystallinity increased with increasing doping. They thought that the dopant did not interact chemically but only physically dispersed [24]. In another study, Rostami et al. obtained polycaprolactone/polyacrylic acid/graphene oxide composite nanofibers. In their study, they showed that when PAA/GO was added to the PCL matrix, the intensity of the peaks increased considerably, thus demonstrating the appropriate compatibility and the effect of PAA/GO on increasing the crystallinity and phase composition of nanofibers. They reported an increase in the amount of crystallinity by adding GO to the PCL composition [35]. The Debye–Scherrer equation was used to determine the crystallite size of the polymer composite including mix and WO_3 additions based on the findings of X-ray measurements. The average crystallite size is calculated using the full width at half maximum (FWHM/β) value derived from the X-ray curve. Below is this equation [39, 40].

$$D = \frac{K\lambda}{\beta \cos \theta}$$

λ is the wavelength of X-ray radiation (CuKα = 0.1541 nm), β is the full width at half maximum (FWHM) of dense and broad peaks, θ is the Bragg or diffraction angle in radians, D is the crystallite size (nm), and k is a constant (value: 0.94) [40, 41]. Using this formula, the crystallite sizes for the PVC-PCL mix base sample and the PVC-PCL polymer composites with 15 % WO_3 addition were 62.68 Å and 171.51 Å, respectively. As the amount of tungsten oxide additive with crystalline properties increases, the crystalline density within the polymer matrix containing amorphous polymers increases [42].

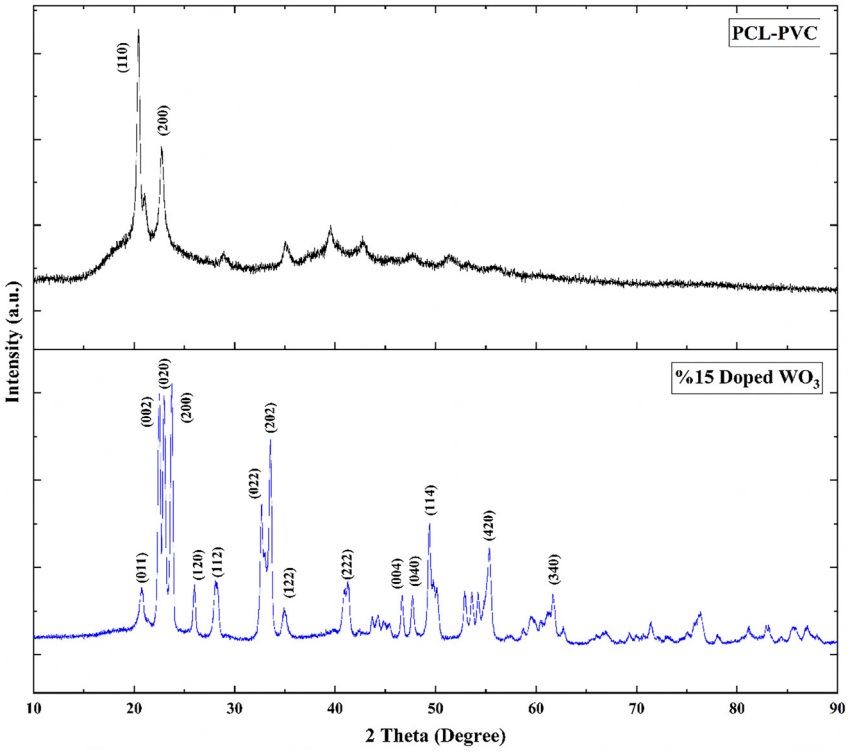

Figure 3: XRD spectra of PVC-PCL blend and 15 % WO_3 doped composites.

Peak width relies on 2θ, and the size and stress-induced peak broadening are assessed independently in the W–H approach, which assesses X-ray peak broadening brought on by the finite size of the coherent scattering zone and internal stress forming within the material [30]. Stress-induced peak broadening in X-ray diffraction is caused by lattice distortion and crystal flaws. The following relationship can be used to compute stress (ε) [43].

$$\varepsilon = \frac{\beta_{hkl}}{4\tan\theta}$$

The calculated ε values for the polymer blend and the composite containing 15 % WO_3 were found to be 0.0725 and 0.0205, respectively. The addition of tungsten oxide to the blend has reduced the microstress value. This result indicates that the additive material causes a decrease in dislocation within the blend, which is the matrix [44].

SEM images taken to show the microstructure of tungsten oxide doped PVC-PCL polymeric composites are given in Figure 4. In order to obtain a clear image during the measurement, the samples were coated with a layer of gold to

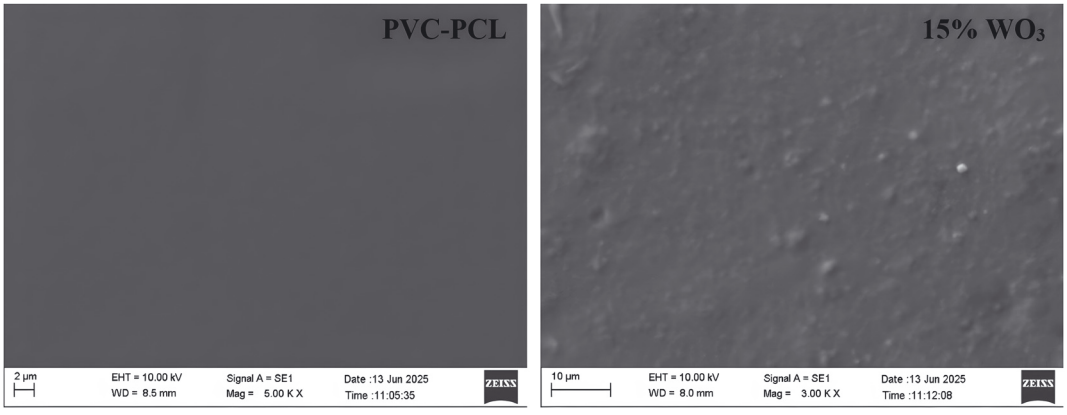

Figure 4: SEM images of PVC-PCL blend and 15 % WO_3 doped composites.

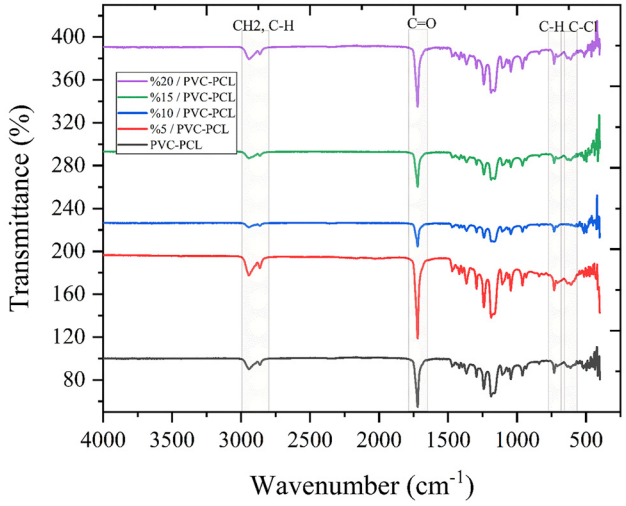

Figure 5: ATR-FTIR spectra of PVC-PCL composite.

increase the conductivity. It can be said that the increase in WO_3 concentration leads to a decrease in surface roughness due to the increase in composite crystallinity. Furthermore, Tungsten Oxide shows a homogeneous distribution within the structure. The measurements show that the surface of the sample is smooth, with small voids and grain clusters merging smoothly. In a similar study, Naveen Kumar et al. reported that in the SEM images of the WO_3 structure formed as a thin film, tungsten oxide is evenly distributed throughout the film and there are some irregularities on the surface, grain boundaries, defects or porosity.

In Figure 5, ATR-FTIR spectra of PVC-PCL matrix nanocomposite films are given. When the characteristic bands specific to polyvinyl chloride (PVC) and poly(ε-caprolactone) (PCL) polymers are examined, stretching vibrations corresponding to acyclic CH_2 and CH groups belonging to the PCL structure are clearly seen around 2,916 cm^{-1} and 2,848 cm^{-1}. The distinct peak observed at approximately 1,720 cm^{-1} shows the C=O (carbonyl) stretching vibration belonging to the ester group of PCL. This band is one of the basic characteristics confirming the existence of PCL. The characteristic bands of PVC are especially concentrated in the range of 1,250–600 cm^{-1}. The bands around 1,330–1,425 cm^{-1} correspond to C–H bending vibrations; The bands in the range of 960–830 cm^{-1} indicate deformation vibrations of –(CHCl)– groups [45]. Especially the absorption in the 610–650 cm^{-1} region represents C–Cl stretching vibrations and is one of the distinctive regions on the spectrum of PVC. Similar results were obtained in our previous studies. As the additive ratio increased, intensity changes were observed especially in the carbonyl region (approximately 1,720 cm^{-1}) and C–Cl vibration regions [46–48]. This indicates that the additive interacts physically or chemically with the polymer matrix. The increase and shifts in the peak intensity, especially in the 15 % and 20 % bands, indicate that these interactions have become more pronounced. In addition, the presence of the additive causes some new bands to appear in the spectrum or the intensity of existing bands to change, signaling structural arrangements. The C=O band in PCL is sensitive to both crystalline and amorphous phases; an increase in the relative strength of the ∼1,730–1,735 cm^{-1} (amorphous) and ∼1,718–1,722 cm^{-1} (crystalline) components indicates increased crystallinity/interaction. According to a study by K. Phillipson et al., a little downward shift and narrowing of the carbonyl band at 15–20 % doping suggests increased local order and a strengthening of the interfacial interaction (like dipole-dipole or H-bonding) with the carbonyl groups [49]. Literature has shown that dipole-dipole/donor-acceptor interactions between the carbonyl groups of PCL and the C–Cl/CH–Cl groups of PVC induce miscibility and band shifts; this is consistent with the downward shift of the carbonyl band and changes in intensity in the C–Cl region [50].

The shape memory effect of the sample added to the blend obtained from PVC (polyvinyl chloride) and PCL (poly(ε-caprolactone)) polymers at a rate of 5 % WO_3 was investigated and schematized in Figure 6. First, it is necessary to heat the material to the softening temperature in order to shape it. The sample cut to certain dimensions was immersed in water for approximately (∼60 °C). The softening temperature is also known as the glass transition temperature (T_g). The softened sample was given its temporary shape and immersed at approximately ∼0 °C and fixed. Subsequently, the segmental mobility of the chains increased when the sample was heated again at ∼60 °C and the structure returned to its original shape. This clearly shows that the PVC-PCL blend exhibits a heat-induced shape memory effect. The amorphous structure of PVC and the semi-crystalline properties of PCL are important parameters affecting both the formability and recycling behavior in this blend system. PCL's low melting temperature (∼60 °C) makes it possible to perform shape memory cycling in the low temperature range [46, 48]. In addition, PVC's rigid structure contributes to the temporary shape fixation. Such blend structures have a wide range of application potential, from biomedical fields to smart textiles [51, 52].

The optoelectronic properties of the prepared PVC-PCL blend and WO_3 doped composites were characterized using UV–Vis spectroscopy. The interaction of light photons with the composite structure results in an optical spectrum. Absorbance and optical band gaps were analyzed to study the optical properties of polymeric blends. The absorption

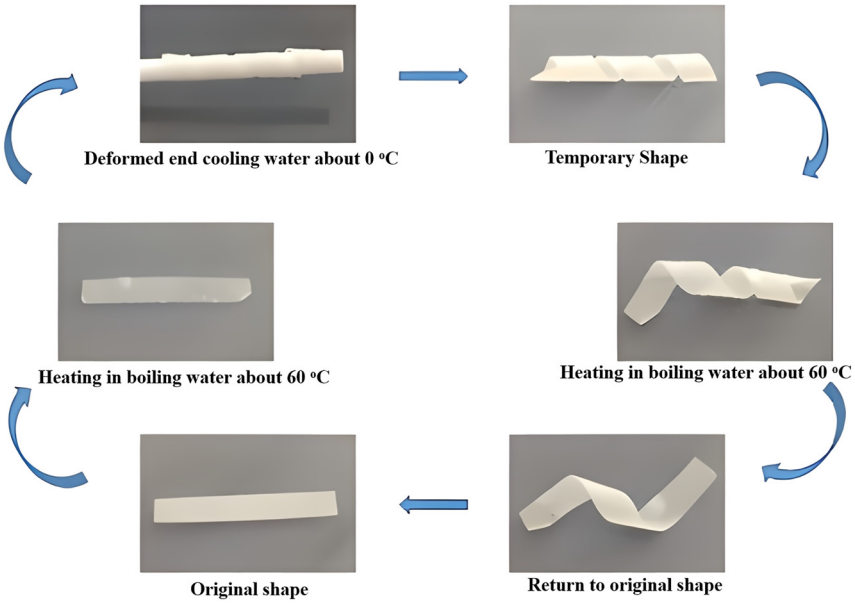

Figure 6: The shape memory effect of PVC-PCL composite.

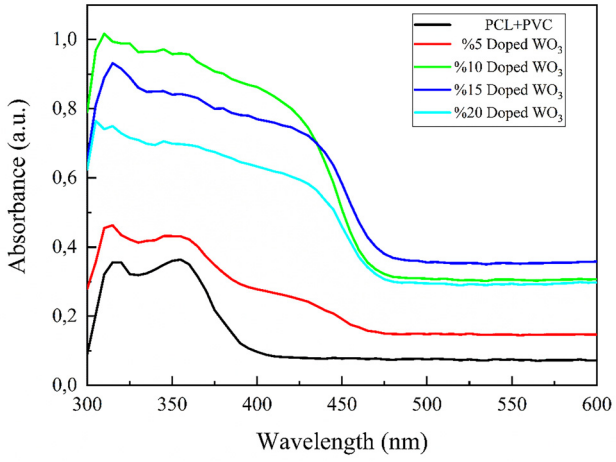

Figure 7: The optical properties of PVC-PCL composite.

spectra of PVC-PCL blend and WO_3 doped composites were taken between 300 and 600 nm wavelengths and shown in Figure 7. On average, high absorption spectra are observed in the UV region below 475 nm and low absorption spectra are observed in the visible region above 475 nm. Therefore, an optical absorption edge around 475 nm is emphasized.

The optical energy range of materials is another area that requires further research because it is crucial to the design of optical devices. The band gap energy, also known as the excitation energy to jump electrons from the valence band to the conduction band, is the energy difference between an atom's low and high energy states. Stated differently, the energy needed for an electron to transition between different energy states is known as the band gap. This transition can take place when incoming light photons interact with material electrons. In generally, In general, two types of transition can occur: direct and indirect. A direct transition is the process by which an electron moves to a higher band while maintaining the same wave vector k value, or momentum. The transition is referred to as a permissive direct transition when the photon's extremely little momentum has no bearing on momentum conservation. The transition is referred to as a forbidden direct transition when the photon momentum is not insignificant during the process. The process by which an electron changes momentum and moves from one band to another is known as an indirect transition. In order to conservation of momentum throughout the transition, a photon is either emitted or absorbed. Once more, the transition is referred to as a permissive indirect transition if the photon momentum can be ignored during the process, and a forbidden indirect transition if it cannot. Forbidden transitions are often far less common [53]. The optical band gap of the synthesized samples is given in Figure 8. The energy required to excite the electrons required to create electron/hole pairs varies depending on the semiconductor material. The band gap energy for the WO_3 semiconductor is between 2.6 and 2.8 eV [17]. Tauc's model is the most widely used for calculating energy values. In this model, the incident photon energy $h\nu$ is linked to the absorption coefficient α. The band gap of WO_3 doped polymeric composites is determined by the following equation,

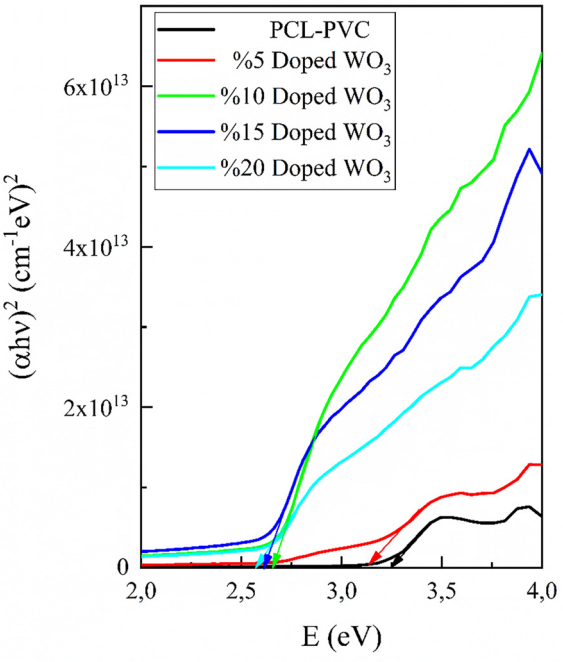

Figure 8: $(\alpha h\nu)^2 - h\nu$ graphs of the PVC-PCL composite.

$$(\alpha h\nu)^n = A(h\nu - E_g)$$

Here E_g is the band gap energy, h is the Planck constant, A is the constant and n is the transition type of the synthesized materials [53–55]. For permitted direct, permitted indirect, and banned direct transitions, the term n has values of 0.5, 2, 1.5, and 3, respectively. One type of transition is distinguished from another by a specific energy gap value. The band gaps of the prepared materials are given in Table 1. According to these results, which are consistent with the literature, the optical band gap decreases with increasing WO_3. Ahlam I. Al-Sulami and colleagues prepared PMMA/PANI-WO_3 nanocomposites and demonstrated that in their optical studies, there was a significant decrease in the band gap from 3.80 eV for pure PMMA/PANI to 3.18 eV at the highest WO_3 loading, accompanied by an improved refractive index [56]. This is due to the increase in the conductivity and the increase in the crystallite size, which is also indicated by the XRD results.

Table 1: Calculated optical band gaps of WO_3 doped polymeric composites.

Samples	E_g (eV)
PVC-PCL	3.25
%5 WO_3	3.14
%10 WO_3	2.66
%15 WO_3	2.62
%20 WO_3	2.60

The energy breadth of localized tail states inside the forbidden band gap is known as the Urbach energy (E_u), and it offers important information about the level of disorder and the existence of structural flaws in a material's electrical and optical characteristics [57]. Urbach energy, sometimes referred to as Urbach tail, is thought to be a significant and dependable instrument for examining the structural properties of polymeric materials. It allows us to identify and describe the degree of fault present in the band gap of these materials. Furthermore, a knowledge of disordered materials' electrical transport properties depends on an understanding of the E_u present in those materials. Band tail states in amorphous materials are known to originate from network strains severe enough to push the states into the forbidden gap. Such tails decrease exponentially in the gap. Implying that the polymers are gradually getting more amorphous [58]. The width of the Urbach energy is expressed by the equation given below;

$$E_U = \left(\frac{dln(\alpha)}{d(h\nu)}\right)^{-1}$$

The Urbach energy is given by E_u, the absorption coefficient by α, and the photon energy by $h\nu$ [59]. It is clear that when the concentration of metal complexes increases, the Urbach energy increases from 0.24 to 0.42. As the tungsten oxide doping ratio increases, the Urbach energies are calculated to be 0.24, 0.27, 0.34, 0.35 and 0.42 eV, respectively. This hints at a greater amorphous phase in polymer composite samples. The increased energy tails will cause the band structure of the composites to become defective and chaotic. This observation also suggests that additional localized states were created within the restricted energy gap. PVC-PCL's clean polymer structure and, as a result, its greater energy gap are directly related to its smaller energy tail width. It is clear that as the concentration of the metal complex increases, the Urbach energy achieves its maximum and the polymer's bandgap reaches its minimal value. The lowering of the bandgap in polymer composites of thin films can be readily explained by the presence of localized defect states in the bandgap energy near the valence band maximum and conduction band minimum. A localized situation in the material caused the Urbach energy to rise, increasing the disorder in the composite film The calculated Urbach energy graph for each prepared sample is given in Figure 9. The higher level of structural disorder and defect states in the nanocomposites is reflected in this rise. Consequently, because these states promote sub-band

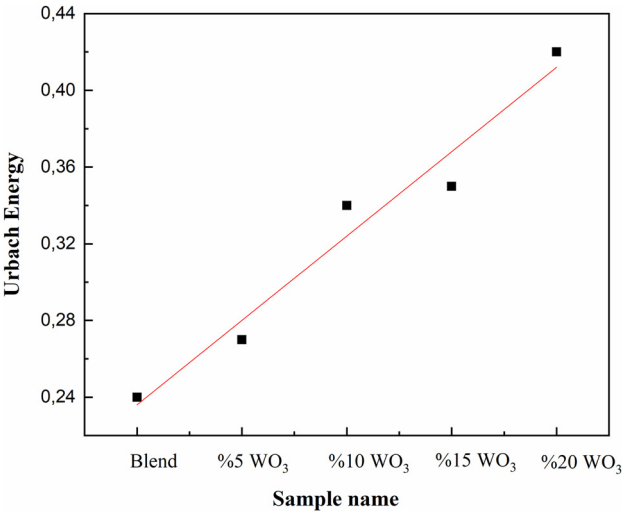

Figure 9: Urbach energy- sample name graphs of the PVC-PCL composite.

gap transitions, the creation of more localized states within the band gap lowers the optical band gap. This correlation demonstrates how significantly the electrical structure and optical performance of the PVC-PCL matrix are impacted by the addition of nanoparticles [57].

4 Conclusions

In this study, PVC-PCL-based nanocomposites doped with different concentrations of tungsten oxide (WO_3) were successfully fabricated and systematically characterized to investigate the impact of WO_3 incorporation on their structural, thermal, optical, and morphological properties. The comprehensive analyses demonstrate that the addition of WO_3 nanoparticles significantly alters the physicochemical behavior of the polymer matrix. Thermal analyses (DSC and TGA) revealed that increasing WO_3 content reduced the melting enthalpy (ΔH_m) and suppressed the crystallinity of the PCL domains within the matrix, implying a strong polymer-filler interaction that restricted chain mobility. Meanwhile, the TGA results confirmed a notable improvement in thermal stability, where the 20 wt% WO_3 sample showed the highest degradation resistance and residual mass. This enhancement is attributed to the excellent heat tolerance and barrier effect of the inorganic WO_3 phase, which effectively delays polymer chain decomposition. Structural characterization via XRD confirmed the semi-crystalline nature of PCL and the amorphous character of PVC, while the incorporation of WO_3 led to an increase in crystallinity with sharper, more intense diffraction peaks. The reduced microstrain values indicate that WO_3 contributes to lattice stabilization and defect minimization. SEM analyses further demonstrated homogeneous dispersion of WO_3 nanoparticles, smoother morphology, and increased surface uniformity, all of which support the improved crystalline structure. FTIR results confirmed physical and possible chemical interactions between WO_3 and the polymer matrix through shifts and intensity changes in C=O and C–Cl bands, consistent with dipole–dipole and hydrogen-bonding mechanisms. Additionally, the 5 % WO_3-doped composite exhibited a distinct shape memory effect, demonstrating reversible deformation around 60 °C due to the synergistic behavior between the flexible PCL phase and the rigid PVC component.

The optical analyses indicated a clear redshift in absorption edge and a systematic decrease in optical band gap from 3.25 eV (pure blend) to 2.60 eV (20 wt% WO_3). This band gap narrowing implies enhanced electronic conductivity and photon–electron interaction, thereby improving the optoelectronic potential of the material. Such properties make these composites suitable candidates for use in flexible optoelectronic devices, UV-protective coatings, electrochromic and sensing applications, and thermally stable dielectric films. Overall, the integration of WO_3 into the PVC-PCL matrix successfully enhanced the thermal durability, optical response, and microstructural order, suggesting that WO_3-doped smart polymer composites represent an environmentally friendly, cost-effective, and multifunctional material platform for next-generation optical and electronic technologies.

Funding information: The authors state no funding involved.

Author contribution: All authors contributed to the study's conception and design. Material preparation, data collection, and analysis were performed by Handan Aydin and Ecem Ozen Oner. The first draft of the manuscript was written by Cihat Aydin and all authors commented on previous versions of the manuscript. All authors have accepted responsibility for the entire content of this manuscript and approved its submission.

Conflict of interest: The authors state no conflict of interest.

Data availability statement: All data generated or analysed during this study are included in this published article.

References

1. Bora PJ, Gupta S, Pecharsky VK, Vinoy K, Ramamurthy PC, Hadimani RL. Enhancement of microwave absorption bandwidth

of polymer blend using ferromagnetic gadolinium silicide nanoparticles. Mater Lett 2019;252:178–81.
2. Yaseen M, Khattak MAK, Khan A, Bibi S, Bououdina M, Usman M, et al. State-of-the-art electrochromic thin films devices, fabrication techniques and applications: a review. Nanocomposites 2024;10:1–40.
3. Elwan HA, Mamlouk M, Scott K. A review of proton exchange membranes based on protic ionic liquid/polymer blends for polymer electrolyte membrane fuel cells. J Power Sources 2021;484:229197.
4. Zhang S, Bunz UH, Bucknall DG. Chromatic conductive polymer nanocomposites of poly (p-phenylene ethynylene) s and single-walled carbon nanotubes. J Compos Sci 2021;5:158.
5. Hou X, Zhang Y, Yin Z, Zhang J. High-k dual crosslinkable polymer nanocomposite dielectrics based on P (MMA-co-HEMA)/BaTiO3 for film capacitors. J Polym Res 2024;31:10.
6. El-Mahalawy AM, Abdrabou MM, Mansour S, Ali FM. Mechanistic exploration of charge transport and photosensitivity of metal/polymer/semiconductor (MPS) junction for sensitive light detection applications. J Mater Sci Mater Electron 2023;34:2313.
7. Gouda M, Khalaf MM, Taleb MFA, Alali I, Abd El-Lateef HM. Development of WO3: PVP: PEG hybrid nanocomposite thin films for optoelectronics applications: structural, optical, and photoelectrical properties investigations. Surf Interfaces 2025;64:106434.
8. Sathishkumar T, Rajeshkumar L, Rajeshkumar G, Sanjay M, Siengchin S, Thakrishnan N, editors. Improving the mechanical properties of jute fiber woven mat reinforced epoxy composites with addition of zinc oxide filler. E3S web of conferences. EDP Sciences; 2022.
9. Algethami N, Rajeh A, Ragab H, Tarabiah A, Gami F. Characterization, optical, and electrical properties of chitosan/polyacrylamide blend doped silver nanoparticles. J Mater Sci Mater Electron 2022;33:10645–56.
10. Harito C, Bavykin DV, Yuliarto B, Dipojono HK, Walsh FC. Polymer nanocomposites having a high filler content: synthesis, structures, properties, and applications. Nanoscale 2019;11:4653–82.
11. Abdelhameed D, Morsi M, Elsisi ME. Impact of CoCl2 on the structural, morphological, optical, and magnetic properties of PCL/PVC blend for advanced spintronic/optoelectronic applications. Ceram Int 2025;51:18713–22.
12. Mijangos C, Calafel I, Santamaría A. Poly (vinyl chloride), a historical polymer still evolving. Polymer 2023;266:125610.
13. Bahmani S, Ghahramani M, Ebrahimi H. Synthesis of poly (vinyl chloride)-g-(poly (hydroxyethyl acrylate)-g-polycaprolactone) plasticizer by sequential of ATRP and ring-opening polymerization. Polym Bull 2025;82:1–19.
14. Morgan AB, Mukhopadhyay P. A targeted review of bio-derived plasticizers with flame retardant functionality used in PVC. J Mater Sci 2022;57:7155–72.
15. Zhang X-P, Zhao J, Wang X-H, Chen Y, Li H-C, Yang L. Highly efficient flame-retardant plasticizers for flexible poly (vinyl chloride) via the synergism of integrated isocyanurate, DOPO and poly (ε-caprolactone). Chem Eng J 2025;510:161658.
16. Al-Mhyawi SR, Al-Sulami AI, AlSulami FMH, Aldahiri RH, Alsabban MM, Mosa FMA, et al. Preparation and modulating of the thermal, optical, dielectric, and electrical properties of PCL/PMMA-NiO/SnO2 nanocomposites for energy storage devices. Ceram Int 2025;51:32623–36.
17. Elabbasy MT, Almarshadi FA, Alshammari MH, Domyati D, El-Morsy M. Synthesis and characterization of polystyrene with embedded WO3/Te2O4 nanoparticles and carbon nanotubes to utilize as antibacterial and wound healing biomaterial. Mater Chem Phys 2025;344:131094.
18. Alhazime AA. Synthesis, characterization, optical, conductivity, and dielectric performance of polymer nanocomposites based on polymethyl methacrylate/polyvinylidene fluoride and WO3 for energy storage device. Ceram Int 2025;51:26547–55.
19. Almehmadi SJ, Alruqi AB, Alsalmah HA, Farea M, Masmali N, Al-Sulami AI, et al. Improving the optical, photoluminescence, and electrical properties of PEO/NaAlg-WO3 nanocomposites for optoelectronic and nanodielectric applications. J Mater Res Technol 2023;26:2310–8.
20. Dhatarwal P, Sengwa R. Enhanced dielectric properties of the ZnO and TiO2 nanoparticles dispersed poly (vinyl pyrrolidone) matrix-based nanocomposites. J Macromol Sci B 2020;59:853–66.
21. Jeon D, Kim N, Bae S, Han Y, Ryu J. WO3/conducting polymer heterojunction photoanodes for efficient and stable photoelectrochemical water splitting. ACS Appl Mater Interfaces 2018;10:8036–44.
22. Alzahrani HS, Al-Sulami AI, Alsulami QA, Rajeh A. A systematic study of structural, conductivity, linear, and nonlinear optical properties of PEO/PVA-MWCNTs/ZnO nanocomposites films for optoelectronic applications. Opt Mater 2022;133:112900.
23. Kalanur SS. Structural, optical, band edge and enhanced photoelectrochemical water splitting properties of tin-doped WO3. Catalysts 2019;9:456.
24. Özen Öner E, Tatar C, Kök M. Synthesis, characterization, optical and gamma shielding properties of La2O3 doped recycled PS-PVC/PCL ternary blend composites. J Polym Environ 2025;33:2920–30.
25. Tatar C, Kök M, Doğru M, Coşkun M, Özen Öner E. Detailed physical property investigation study on ZnO NPs containing waste PS-PLA smart polymeric composites: crystal structure, thermal, optical properties and radiation shielding behavior. Macromol Res 2025:1–11.
26. Masek A, Zaborski M. ENR/PCL polymer biocomposites from renewable resources. C R Chim 2014;17:944–51.
27. Tokiwa Y, Calabia BP, Ugwu CU, Aiba S. Biodegradability of plastics. Int J Mol Sci 2009;10:3722–42.
28. Kök M, Özen Öner E, Coşkun M, Pekdemir ME, Aydoğdu Y. Improving of insulation PS materials with smart PCL and investigation of some physicochemical properties of their blends. J Appl Polym Sci 2025;142:e57490.
29. Daikhi S, Hammani S, Guerziz S, Alsaeedi H, Sayegh S, Bechlany M, et al. Urchin-like WO3 particles form honeycomb-like structured PLA/WO3 nanocomposites with enhanced crystallinity, thermal stability, rheological, and UV-blocking and antifungal activity. Polymers 2024;16:2702.
30. Tomaszewska J, Sterzyński T, Woźniak-Braszak A, Banaszak M. Review of recent developments of glass transition in PVC nanocomposites. Polymers 2021;13:4336.
31. Gedde UW, Hedenqvist MS, Hakkarainen M, Nilsson F, Das O. Applied polymer science. Cham, Switzerland: Springer; 2021.
32. Prasad RC. Composites, science, and technology. New Delhi, India: New Age International; 2000.
33. Taşgin Y, Pekdemir ME, Yilmaz M, Kanca MS, Kök M. Physical and shielding properties of Er2O3 rare earth oxide

compound content on PCL/PEG blend. Polym Bull 2024;81:2915—31.
34. Campos AD, Marconato JC, Martins-Franchetti SM. The influence of soil and landfill leachate microorganisms in the degradation of PVC/PCL films cast from DMF. Polímeros 2012;22:220—7.
35. Rostami M, Jahed-Khaniki G, Molaee-Aghaee E, Shariatifar N, Sani MA, Azami M, et al. Polycaprolactone/polyacrylic acid/graphene oxide composite nanofibers as a highly efficient sorbent to remove lead toxic metal from drinking water and apple juice. Sci Rep 2024;14:4372.
36. Ali S, Khatri Z, Oh KW, Kim I-S, Kim SH. Preparation and characterization of hybrid polycaprolactone/cellulose ultrafine fibers via electrospinning. Macromol Res 2014;22:562—8.
37. Kök M, Mohammed KS, Öner EÖ, Qader IN, Aydoğdu Y. Exploring the impact of Dy2O3 nanoparticles on the physical characteristics of poly (lactic acid) and polyhydroxyalkanoate composites. J Polym Res 2025;32:3.
38. Hatel R, Baitoul M. Nanostructured tungsten trioxide (WO3): synthesis, structural and morphological investigations. J Phys Conf 2019;1292:012014.
39. Basak M, Rahman ML, Ahmed MF, Biswas B, Sharmin N. The use of X-ray diffraction peak profile analysis to determine the structural parameters of cobalt ferrite nanoparticles using Debye-Scherrer, Williamson-Hall, Halder-Wagner and size-strain plot: different precipitating agent approach. J Alloys Compd 2022;895:162694.
40. Sariateş D, Kök M. Carbide-reinforced NiMnSn shape memory alloy composites: fabrication and thermal, microstructural, magnetic properties. J Therm Anal Calorim 2025:1—8.
41. Wulandari NP, Choerullah A, Afandi AN, Malek NANN, Mufti N, Sunaryono S. Influence of ZnO composition on the physical properties of Mn0. 75Fe2. 25O4/ZnO/PVP/PABS nanocomposites and their application as photodetector materials. ECS J Solid State Sci Technol 2025;14:104001.
42. Qader IN, Kök M, Mohammed KS, Coskun M, Öner EÖ, Aydoğdu Y. Development of a PLA/PHA-TiO_2 polymer blend with improved physicochemical and thermal properties. J Polym Environ 2025:1—13.
43. Samanta P. Effect of microstrain on the crystallite size of ZnO nanoparticles: X-ray peak profile and Rietveld analysis. Next Mater 2025;8:100841.
44. Strunz P, Kunčická L, Beran P, Kocich R, Hervoches C. Correlating microstrain and activated slip systems with mechanical properties within rotary swaged WNiCo pseudoalloy. Materials 2020;13:208.
45. Raftari R, Maghsoud Z. Evaluation of the compressible regular solution model predictions via rheologically determined phase diagram for polyvinylchloride/polycaprolactone blend. Polym Bull 2023;80:3227—46.
46. Koek M, Pekdemir ME, Öner EÖ, Coşkun M, Hekim S. MWCNT nanocomposite films prepared using different ratios of PVC/PCL: combined FT-IR/DFT, thermal and shape memory properties. J Mol Struct 2023;1279:134989.
47. Pekdemir M, Qader IN, Aydogdu Y, Coşkun M. Exploring of polyvinylchloride/silicon carbide nanocomposites containing different amounts of SiC nanoparticles. El-Cezeri 2021;8:1395—404.
48. Pekdemir ME, Öner E, Kök M, Qader IN. Thermal behavior and shape memory properties of PCL blends film with PVC and PMMA polymers. Iran Polym J (Engl Ed) 2021;30:633—41.
49. Phillipson K, Hay J, Jenkins M. Thermal analysis FTIR spectroscopy of poly (ε-caprolactone). Thermochim Acta 2014;595:74—82.
50. Mareau VH, Prud'Homme RE. Growth rates and morphologies of miscible PCL/PVC blend thin and thick films. Macromolecules 2003;36:675—84.
51. Zhao Q, Qi HJ, Xie T. Recent progress in shape memory polymer: new behavior, enabling materials, and mechanistic understanding. Prog Polym Sci 2015;49:79—120.
52. Liu Y, Du H, Liu L, Leng J. Shape memory polymers and their composites in aerospace applications: a review. Smart Mater Struct 2014;23:023001.
53. Elkattan M, Gad M. Investigation of the absorption edge and the optical bandgap of PVA/PVP-based thin films. J Electron Mater 2025;54:831—47.
54. Alshammari DA. Synthesis of Ag and Gd Co-doped LaCoO3: tuning the optical bandgap through quantum confinement effect for outstanding photocatalytic activity. Ceram Int 2025;51:3595—606.
55. Alqarni MA, Rajeh A. Optimizing the structural, optical, dielectric, and electrical properties of polyvinyl alcohol/polyvinyl pyrrolidone/zinc manganite nanocomposites for optical and energy storage applications. Results Phys 2024;67:108045.
56. Al-Sulami AI, Elamin NY, Aldosari E, Farea M, Alzahrani SS, Al-Harthi AM, et al. Tunable band gap and ionic conductivity in PMMA and PANI blend with WO_3 nanocomposites for optoelectronics and energy storage devices. Sci Rep 2025;15:34543.
57. Alhazime AA. Enhancing the optical behavior of PMMA/PVDF composites using hybrid GO/SiO_2 nanofillers. Inorg Chem Commun 2025;182:115664.
58. Mohammed HA, Mohammed PA, Aziz SB. Investigation of optical band gap in PEO-based polymer composites doped with green-synthesized metal complexes using various models. RSC Adv 2025;15:23319—41.
59. Mamand DM, Hussen SA, Aziz SB. Drude-Lorentz classical oscillator model and Tauc's approach to study the localized density of states and energy band gap of polymer composites based on chitosan integrated with green synthesized Pb-metal complexes: improvement of linear and non-linear optical parameters. Int J Biol Macromol 2025;312:143978.